CrystEngComm

PAPER

View Article Online
View Journal | View Issue

Cite this: *CrystEngComm*, 2017, **19**, 4345

$^{sp^2}$CH···Cl hydrogen bond in the conformational polymorphism of 4-chloro-phenylanthranilic acid†

Meng Liu, [a] Chuming Yin, [a] Peng Chen, [a] Mingtao Zhang, [b] Sean Parkin, [d] Panpan Zhou, [c] Tonglei Li, [b] Faquan Yu *[a] and Sihui Long *[a]

Received 24th April 2017,
Accepted 7th July 2017

DOI: 10.1039/c7ce00772h

rsc.li/crystengcomm

Chlorine can participate in numerous interactions such as halogen bonding, hydrogen bonding, and London dispersion in the solid state. In this work, we report the influence of a chlorine substituent on the polymorphism of a potential anticancer drug, 4-chloro-phenylanthranilic acid (CPAA). Three polymorphs have been discovered for this compound, and the three forms were characterized by single-crystal X-ray diffraction, power X-ray diffraction (PXRD), FT-IR, and Raman spectroscopy. Both conformational flexibility of the molecule and the $^{sp^2}$CH···Cl hydrogen bond seem to lead to the polymorphism of the system. The phase behavior was investigated by differential scanning calorimetry (DSC), with the conclusion that form II converts to III upon heating. A conformational scan shows the conformational minima corresponds to the conformers existing in the polymorphs. Lattice energy calculations show energies of −106.70, −104.72, and −194.42 kJ mol^{-1} for forms I to III, providing information on relative stability for each form. Hirshfeld analysis revealed that intermolecular interactions such as H···H, C···H, H···Cl, and H···O contribute to the stability of the crystal forms.

1. Introduction

Non-steroidal anti-inflammatory drugs (NSAIDs) are essential medicines in everyday life since some of them also possess antipyretic, analgesic, and antirheumatic properties in addition to anti-inflammatory effects.[1] Classic NSAIDs include salicylic acid derivatives, pyrozolones, arylalkanoic acids [aryl- and heteroarylacetic acids, aryl- and heteroarylpropionic acids, and *N*-arylanthranilic acids (a.k.a. fenamic acids)], and oxicams.

Fenamic acids (FAs) are nitrogen isosteres of salicylic acid. Representative fenamic acid NSAIDs include mefenamic acid, meclofenamic acid, chlofenamic acid, tolfenamic acid, flufenamic acid, niflumic acid, clonixin, and flunixin. These compounds are potent cyclooxygenase (COX) inhibitors, which lend them anti-inflammatory properties. Like other NSAIDs, they can also act as analgesics and antirheumatics. Recently, FAs have also been investigated as therapeutics for neurodegenerative and amyloid diseases as well as cancer, and some have shown great promise.[2–4] In addition, FAs are also synthetic precursors to acridones and acridines, which present bioactive properties such as anti HIV, anticancer, antibacterial, antifungal, and antimalarial activities.[5]

4-Chloro-2-phenylanthranilic acid (CPAA) (Scheme 1) is an FA with a modest COX inhibitory effect due to the presence of the chlorine atom on the anthranilic acid moiety [structure–activity relationship (SAR) studies of FAs indicate that substitution on the anthranilic acid aromatic ring makes them weak COX inhibitors].[6,7] Although it has poor anti-inflammatory properties, it shows good inhibitory effects on the aldol-keto reductase (AKR), which likely is involved in the development of hormone-dependent breast cancer.[8] It was also investigated as a Cl$^-$-channel blocker in chloride transporting epithelia, which has ramifications in myotonia such as Thomsen's and Becker's disease, cystic fibrosis, hereditary calculus of kidney, and type 3 Bartter's syndrome.[9] Its affinity to bovine albumin was also studied to help design better FA drugs.[10]

Fenamic acids are diarylamines and conformationally flexible, which makes them prone to show polymorphism, *i.e.*,

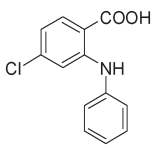

Scheme 1 Structure of 4-chloro-2-phenylanthranilic acid.

[a] *Key Laboratory for Green Chemical Process of Ministry of Education, School of Chemical Engineering and Pharmacy, Wuhan Institute of Technology, Wuhan, Hubei, China. E-mail: fyuwucn@gmail.com, sihuilong@wit.edu.cn, longsihui@yahoo.com; Tel: +(027) 87194980, +(86) 15549487318*
[b] *Department of Industrial and Physical Pharmacy, Purdue University, West Lafayette, Indiana, USA*
[c] *Department of Chemistry, Lanzhou University, Lanzhou, Gansu, China*
[d] *Department of Chemistry, University of Kentucky, Lexington, Kentucky, USA*

† CCDC 1545269, 1545271 and 1545272. For crystallographic data in CIF or other electronic format see DOI: 10.1039/c7ce00772h

existing in more than one crystal form.[11] Polymorphism is widely observed in organic compounds, particularly those that are conformationally flexible.[12] Many FAs exhibit polymorphism. For example, two, five, nine, two, and four forms have been found for mefenamic acid,[13] tolfenamic acid,[14] flufenamic acid,[15] niflumic acid,[16] and clonixin,[17] respectively. The existence of nine forms of flufenamic acid is reported to be the current world record for most forms having been structurally characterized by single-crystal X-ray diffraction.[15] Polymorphism is of particular significance in pharmaceuticals because different forms of the same API may have different kinetic, thermodynamic, surface, mechanical, and packaging properties, which can affect clinical formulation and eventual bioavailability.[18,19]

Similar to the classic fenamic acid NSAIDs, CPAA is conformationally flexible. It differs from the well-known FA drugs, which have substituents on the aniline ring, by having the substituent Cl on the anthranilic acid aromatic ring of CPAA instead. Chlorine is known to have steering effect on the spatial arrangement of the molecules due to its participation in halogen bonds.[20–24] Moreover, the carboxylic acid is able to form both a catemer motif and the more common acid–acid dimer.[25] How would the combination of conformational flexibility, variability of carboxylic acid interactions and the presence of Cl on the anthranilic acid aromatic ring influence the polymorphic behavior of CPAA? In this study, we investigate the effect of the substituent, *i.e.*, Cl on the solid-state properties, specifically polymorphism of CPAA. We describe three polymorphs for CPAA, their characterization, phase behavior, and the related theoretical studies.

2. Experimental section

2.1. General

All solvents and reagents were purchased from commercial sources and used as received: 2,4-dichlorobenzoic acid, aniline, and Cu_2O were from Aladdin; Cu, K_2CO_3, 2-ethoxyethanol, and the solvents used for crystal growth were from Sinopharm Chemical Reagent Co., Ltd. The IR, Raman and UV-vis spectra were recorded using an FT-IR Perkin-Elmer LX10-8873, a Thermo Electron DXR Laser Confocal Microscopy Raman Spectrometer, and a Lambda 750 UV/vis/NIR spectrophotometer, respectively. NMR spectra were obtained on a Varian INOVA spectrometer at an observation frequency of 400 MHz. Thermal analyses were performed on an SII DSC 6220 (SEIKO, Japan) apparatus, using a heating rate of 10 °C min^{-1}.

2.2. Synthesis and characterization

Synthesis of CPAA (Scheme 2). 2,4-Dichlorobenzoic acid (2.00 g, 10.0 mmol), aniline (1.02 g, 11.0 mmol), Cu (5.8 mg, 0.9 mmol), Cu_2O (5.8 mg, 0.4 mmol) and K_2CO_3 (2.76 g, 20.0 mmol) were added to a round-bottom flask, followed by addition of 2-ethoxyethanol (13 mL) under nitrogen protection. The resulting mixture was refluxed at 130 °C for 24 h. The hot reaction mixture was poured into 30 mL of room temperature water. The mixture was filtered. The crude product was obtained by precipitation upon acidification of the filtrate with dilute HCl. The product was purified on a silica-gel column using petroleum ether/ethyl acetate (v/v 4 : 1, R_f = 0.50) as eluent. The product was obtained as colorless solid (1.55 g, yield%: 60).

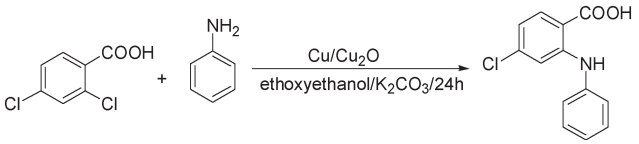

Scheme 2 Synthesis of CPAA.

^{1}HNMR (400 MHz, $CDCl_3$): δ_{ppm} 9.36 (s, 1H), 7.96 (d, 1H), 7.41 (t, 2H), 7.27 (d, 2H), 7.20 (t, 1H) 7.14 (d, 1H), 6.71 (dd, 1H); ^{13}CNMR (100 MHz, $CDCl_3$): δ_{ppm} 173.0, 150.0, 142.0, 139.7, 133.7, 129.6, 125.4, 123.9, 117.4, 113.2, 108.4; IR (KBr, cm^{-1}) 3330 (s), 3036–2500 (s), 1665 (s), 1559 (s), 1498(s), 1416 (s), 1330 (m), 1251 (s), 1156 (s), 1094 (s), 930 (s), 752 (s), 684 (s), 574 (s); MS (ESI): 248.24 (M + 1); mp: 204 °C.

2.3. Crystal growth

The crystal growth method of slow evaporation, slow cooling, and quench cooling was applied for polymorph screening of CPAA. For slow evaporation, the pure compound was dissolved in different solvents, forming saturated solutions at ambient temperature (~22 °C) (Table 1). The solutions were set for slow evaporation in a vibration-free place until single crystals were harvested. As an example, 100 mg of CPAA was added to 10 mL HPLC grade methanol. The mixture was stirred overnight and the remaining solid was removed by pipette filtration. A vial containing the clear solution was covered with perforated parafilm. Slow evaporation led to single crystals in about a week. For slow cooling, a saturated solution in a beaker covered by cover glass was concentrated to 1/3 of the original volume by gentle heating on a hot plate, followed by cooling to room temperature with the heat source turned off. For quench cooling, a supersaturated solution of

Table 1 Crystal growth of CPAA in a variety of solvents

Solvents	Method	Form
MeOH	Slow evaporation	**I**
Hexane	Slow evaporation	**I**
i-PrOH	Slow evaporation	**I**
CH_3CN	Slow evaporation	**I**
Toluene	Slow evaporation	**I**
$CHCl_3$	Slow evaporation	**I**
EtOAc	Slow evaporation	**I**
EtOAc	Slow cooling	**II**
Acetone	Slow evaporation	**II**
Ether	Slow evaporation	**II**
CH_2Cl_2	Quench cooling	**II**
DMSO	Slow evaporation	**II**
THF	Slow evaporation	**II**
DMF	Slow evaporation	**II**
H_2O	Slow evaporation	No crystals formed
Benzene	Slow evaporation	**III**
CH_3COOH	Slow evaporation	**III**

CPAA in CH_2Cl_2 at 40 °C was rapidly cooled in a freezer with a temperature of −20 °C. All crystallization experiments were conducted in an unmodified atmosphere. Each experiment was repeated multiple times. Specifically, forms **I**, **II**, and **III** can be produced in chloroform, methylene chloride, and acetic acid, respectively, and other solvents as well. The identity of the crystals was confirmed by powder X-ray diffraction for tiny, and by single-crystal X-ray diffraction when high-quality single crystals were obtained.

2.4. Crystal structure determination

The crystal structures of all three polymorphs of CPAA were determined by single-crystal X-ray diffraction.

Data collection was carried out at 90 K on a Nonius kappaCCD diffractometer with MoKα radiation (λ = 0.71073 Å).[26] Cell refinement and data reduction were done using SCALEPACK and DENZO-SMN.[27] Structure solution and refinement were carried out using the SHELXS and SHELXL2016 programs, respectively.[28,29]

Powder X-ray diffraction (PXRD) data for each sample were collected on a Rigaku X-ray diffractometer with CuKα radiation (40 kV, 40 mA, λ = 1.5406 Å) between 5.0–50.0° (2θ) at ambient temperatures. The finely ground sample was placed on a quartz plate in an aluminum holder.

2.5. Thermal analyses

Phase behavior for each of the solid forms was studied by differential scanning calorimetry (DSC). The instrument and procedure were aforementioned.

Spectroscopic studies

IR and Raman. For IR spectrum recording, samples were dispersed in KBr pellets. For Raman measurement, samples were compressed in a gold-coated sample holder.

UV-vis. For the UV-vis experiments, solutions (in chloroform, dichloromethane, and acetic acid) were contained in quartz cuvettes. The concentrations of the solutions were 1×10^{-4} mol L^{-1}, 5×10^{-5} mol L^{-1} and 1×10^{-4} mol L^{-1} respectively.

2.6. Computational details

Conformation search. Conformational flexibility potentially derives from three bonds, *i.e.*, C2–C14, C1–N7 and N7–C8 (Fig. 1). However, the double-bond character of C1–N7 (C–C = ∼1.37 Å) precludes rotation, and in spite of the essentially single-bond character for C2–C14 bond (C–C = ∼1.47 Å), the carboxylic acid group in all conformers is coplanar with the aromatic ring (Table 2). Thus, the energy of different conformations of a single CPAA molecule defined solely by the torsion angle, τ (C1–N7–C8–C9) was evaluated with Gaussian 09 (Gaussian, Inc., Wallingford, CT). The molecule was optimized from various initial structures in order to identify the most stable conformation, which was then used for scanning each torsion angle with all bond lengths, bond angles, and other torsion angles fixed. Structural optimization and conformational searches were performed at the B3LYP/6-311+G(d, p) level of theory.

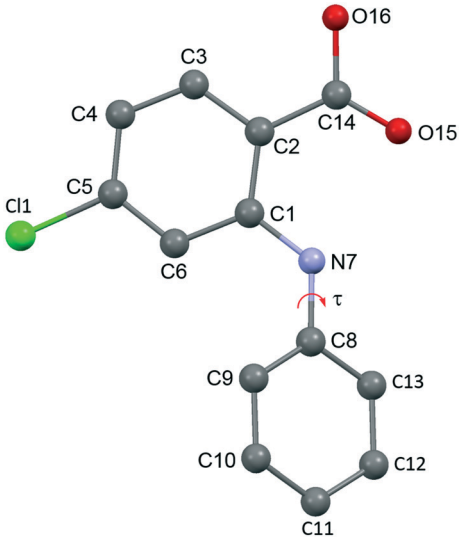

Fig. 1 Labeling of CPAA.

Lattice energy. To calculate lattice energies for each CPAA form, the experimental crystal structures were first optimized with the lattice parameters kept constant. Optimization was conducted by DFT using PW1PW functional with 6-21g** basis sets by Crystal14.[30] Dispersion energy contributions to lattice energies were calculated using the DFT-D3 program of Grimme, with Becke–Johnson damping.[31,32] Basis set superposition error (BSSE) was considered by the counterpoise method.[33] The energy convergence of the optimization and energy calculation was set to 10^{-7} hartree. The root-mean-square (RMS) values for calculation convergence were set to 0.0003 and 0.0012 au for energy gradient and atomic displacement, respectively. All calculations were conducted on a Linux cluster.

Hirshfeld surface analysis. Hirshfeld surface analyses[34,35] were performed with CrystalExplorer (Version 3.1)[36] to further understand the relative contributions to intermolecular interactions by various molecular contacts in the polymorphs.

3. Results and discussion

3.1. Crystal structures

Three polymorphs (**I**, **II**, and **III**) of CPAA have been discovered so far (Fig. 2). Form **I** crystals were obtained as colorless plates from (but not limited to) ethyl acetate, form **II** crystals

Table 2 Bond length of C1–N7 and N7–C8 in the conformers of CPAA

	Bond length (Å)	
Conformer	C1–N7	N7–C8
I-A	1.372	1.420
I-B	1.371	1.421
II-A	1.366	1.426
II-B	1.368	1.416
III	1.376	1.407

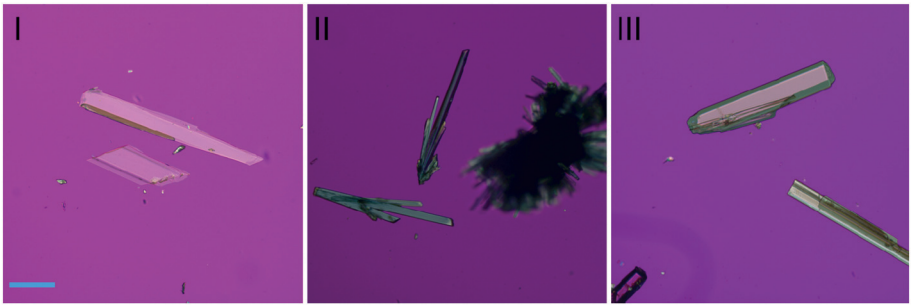

Fig. 2 Crystals of CPAA polymorphs I–III.

were grown as long yellow rods from (but not limited to) acetone and form **III** crystals were harvested as colorless rods from benzene or acetic acid. Structure determination by single-crystal X-ray diffraction found form **I** to be triclinic, space group $P\bar{1}$ (Z = 4); form **II** to be triclinic, space group $P\bar{1}$ (Z = 4); form **III** to be orthorhombic, space group *Pbca* (Z = 8). Crystallographic data for each form are given in Table 3; for complete CIF files, see the ESI.† Careful examination of the crystallographically independent molecules in each of the asymmetric units indicates they are conformationally different, as suggested by the dihedral angle between the two aromatic rings (54.84(5)° for **I**-A and 60.53(5)° for **I**-B in form **I**, 64.43(5)° for **II**-A and 48.99(6)° for **II**-B in form **II**, and 40.76(10)° for form **III**). Conformational variability is readily apparent in a superposition of all five experimental conformations (Fig. 3).

Table 3 Crystallographic data of CPAA polymorphs I–III

	I	II	III
Formula	$C_{13}H_{10}ClNO_2$	$C_{13}H_{10}ClNO_2$	$C_{13}H_{10}ClNO_2$
Formula weight	247.67	247.67	247.67
Crystal size	0.50 × 0.20 × 0.10	0.20 × 0.03 × 0.03	0.40 × 0.10 × 0.10
Crystal system	Triclinic	Triclinic	Orthorhombic
Space group	$P\bar{1}$	$P\bar{1}$	*Pbca*
a/Å	9.9015(2)	8.2249(2)	9.85040(10)
b/Å	10.7701(2)	10.1269(3)	7.4915(2)
c/Å	11.3935(2)	13.7993(4)	31.4272(8)
α/°	90.2523(8)	88.2266(11)	90
β/°	103.8986(8)	85.9540(11)	90
γ/°	102.7160(8)	81.4168(11)	90
Z, Z'	4, 2	4, 2	8, 1
V/Å^3	1148.40(4)	1133.43(5)	2319.15(9)
D_{cal} g^{-1} × cm^{-3}	1.432	1.451	1.419
T/K	90.0(2)	90.0(2)	90.0(2)
Abs coeff (mm^{-1})	0.320	0.324	0.317
F(000)	512	512	1024
θ range (deg)	1.84–27.48	1.48–27.50	1.30–27.47
Limiting indices	$-12 \le h \le 12$ $-13 \le k \le 13$ $-14 \le l \le 14$	$-10 \le h \le 10$ $-13 \le k \le 13$ $-17 \le l \le 17$	$-12 \le h \le 12$ $-9 \le k \le 9$ $-40 \le l \le 40$
Completeness to 2θ	99.9%	99.8%	100.0%
Unique reflections	3681	3265	1420
$R_1[I > 2\sigma(I)]$	0.0405	0.0437	0.0549
wR_2 (all data)	0.1163	0.1017	0.1778

In form **I**, the asymmetric unit consists of two molecules (Z' = 2), each having a twisted conformation with the dihedral angle between the two aromatic rings of 54.84(5)° for molecule A and 60.53(5)° for molecule B. The two molecules form an acid–acid dimer hydrogen-bonding motif ($R_2^2(8)$).[37–39] The intermolecular hydrogen bond has a bond distance and bond angle of 1.674(10) Å and 175.9(2)° for O16B–H16B···O15A, and 1.70(2) Å and 174.2(2)° for O16AH16A···O15B, respectively. Pairs of such dimers further interact *via* weak $^{sp^2}$CH···Cl hydrogen bonds between C12A–H12A and Cl1A (graph set ($R_2^2(18)$)). The bond distance between H12A and Cl1A is 2.930 Å, bond angle of C12A–H12A···Cl1A is 117.36°, and the distance between C12A and Cl1A is 3.471 Å, which is nearly identical with the sum of the van der Waals radii of the two atoms. Cl1B is not involved in hydrogen bond. In addition to the intermolecular hydrogen bonds, an intramolecular hydrogen bond exists between the carboxylic acid carbonyl O and the NH bridging the two aromatic rings, with a bond distance of 1.973(18) Å and bond angle 133.3(2)° for molecule A and 1.951(18) Å and 136.3(2)° for molecule B (Fig. 4).

Similar to form **I**, form **II** has two molecules in the asymmetric unit (Z' = 2), and both molecules show a twisted conformation, with a dihedral angle of 64.43(5)° for molecule A and 48.99(6)° for molecule B. The two molecules also form A–B acid–acid dimers. The intermolecular hydrogen bond

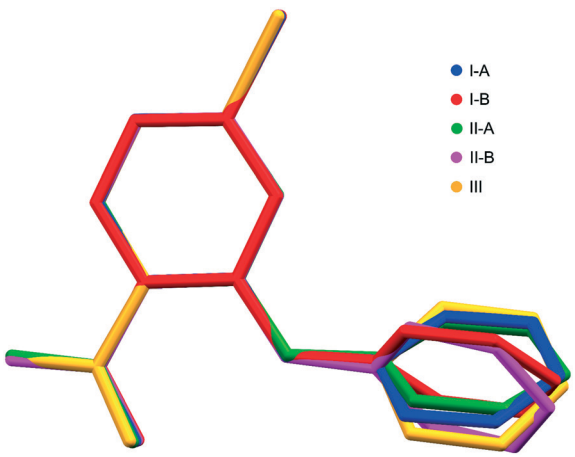

Fig. 3 Superposition of all five molecular conformations in the asymmetric units of the three polymorphs of CPAA.

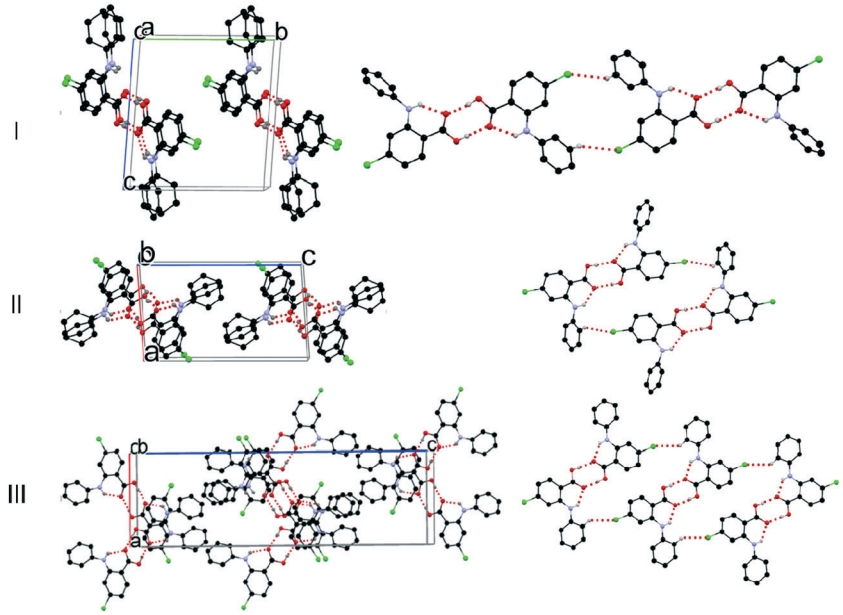

Fig. 4 Crystal packing of I (a), II (b), III (c). For clarity, only intermolecular hydrogen bonds are shown (dotted line).

has a bond distance and bond angle of 1.73(2) Å and 174.6(2)° for O16B–H16B···O15A, and 1.60(2) Å and 176.0(2)° for O16AH16A···O15B, respectively. These acid–acid dimers are further connected by two non-conventional $^{sp^2}$CH···Cl hydrogen bonds between C13B–H13B and Cl1A, forming a dimer of dimers, but in a different manner than **I**. In form **I**, the two $^{sp^2}$C–H···Cl hydrogen bonds help form inversion-related dimer between two molecules and two dimers, and in form **II**, the two $^{sp^2}$C–H···Cl hydrogen bonds only connect two dimers. The bond distance between H13B and Cl1A is 2.870 Å, the bond angle of C13B–H13B···Cl1A is 108.71°, which falls slightly below the preferred minimum hydrogen bond angle of 110°, and the distance between C13B and Cl1A is 3.300 Å, which is less than the sum of the van der Waals radii of C and Cl.[40] Cl1B again is not involved in hydrogen bond. An intramolecular hydrogen bond similar to that in form **I** is formed between the carbonyl O of the carboxylic acid and the anilino NH, with a bond distance of 2.01(2) Å and bond angle 136.2(2)° for molecule A and 1.944(19) Å and 136.8(2)° for molecule B.

The form **III** crystallizes with one molecule in the asymmetric unit. The molecule has a dihedral angle between the two aromatic rings of 40.76(10)°. Inversion-related pairs of molecules form acid–acid homodimers (graph set ($R_2^2(8)$)). The hydrogen bond has a bond distance of 1.76(3) Å and bond angle of 178(3)°. The $^{sp^2}$-CH···Cl weak hydrogen bond between C13–H13 and Cl1 (bond distance of H13 and Cl1 is 2.945 Å, and bond angle of C13–H13···Cl1 is 133.43°) leads to extended dimer tapes due to the participation in hydrogen bonding of the chlorine. The distance between C13 and Cl1 (3.664 (3) Å) is longer than the sum of the van der Waals radii of the two atoms. The intramolecular hydrogen bond has parameters of 1.96(3) Å and 137(2)° (Fig. 4).

Only one crystal form of fenamic acid has been obtained after an exhaustive polymorph screening, and various numbers of polymorphs have been discovered for other substituted FAs. It is inferred that the substituent groups play an important role on the polymorphism of FAs.[14] The three polymorphs of CPAA, therefore, result likely from both the conformation differences of the molecules and the non-conventional $^{sp^2}$CH···Cl hydrogen bonds. The conformational variation and the presence of $^{sp^2}$CH···Cl hydrogen bonds could be mutually dependent. A methyl/Cl exchange should shed light on the structure determining role of chlorine.

3.2. Thermal properties

DSC was conducted to investigate the thermal properties of the three forms, shown in Fig. 5. Form **I** shows only one

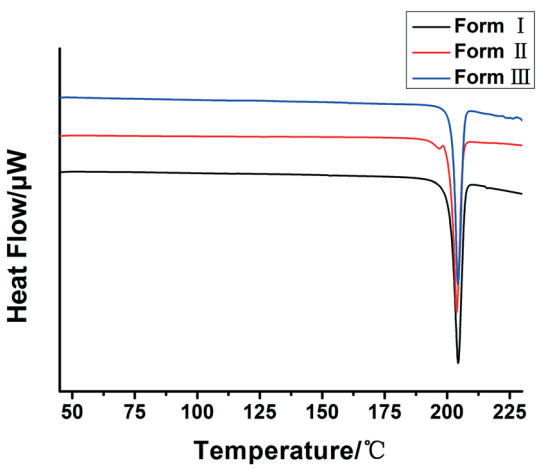

Fig. 5 DSC thermograms of the polymorphs of CPAA.

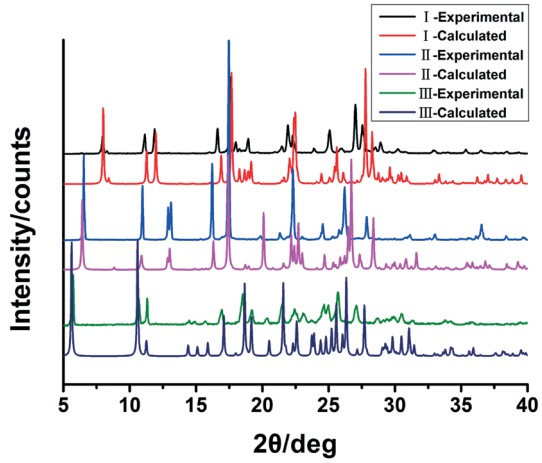

Fig. 6 Experimental and calculated PXRD patterns of the three polymorphs.

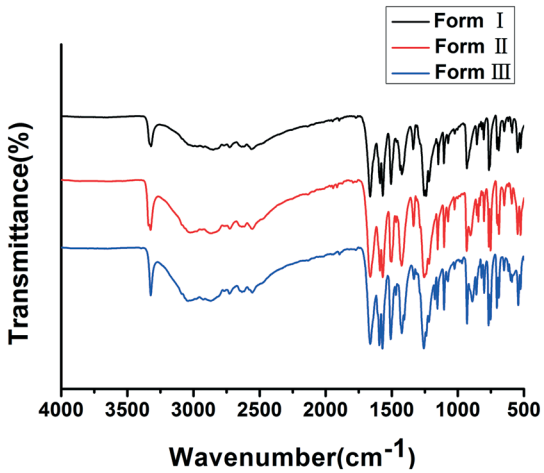

Fig. 7 IR spectra of the three polymorphs.

DSC peak with an onset temperature of 198.5 °C, which is the melting of the crystals. Form **II** has two endothermic DSC peaks. The first, with the onset temperature of 192.5 °C, appears to be a phase transition to a new form that melts at approximately 199.0 °C. Form **III** shows only one peak with an onset temperature of 198.8 °C, which corresponds to the melting of the crystals. Based on the DSC thermograms, we can infer that form **II** converts into form **I** or **III** when heated. As mentioned before, form **I** has a Z' = 2 and form **II** has a Z' = 1 and most of the time, the Z' = 1 form is more stable than the high Z' forms.[41,42] Thus, form **II** likely converts into form **III** instead of form **I**, and there is also a good chance that form **I** also converts into form **III**, yet the energy involved is extremely small. Nevertheless, we cannot rule out the possibility that forms **I** and **III** happen to be isoenergetic.[43,44]

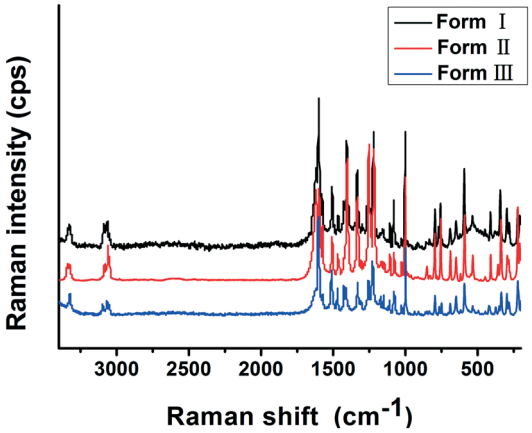

Fig. 8 Raman spectra of CPAA polymorphs.

Fig. 6 shows powder X-ray diffraction patterns of forms **I**, **II**, and **III** collected at room temperature, along with patterns calculated from the single-crystal structures determined at 90 K. The similarity of experimental and calculated patterns for each form indicates the thermodynamic stability at room temperature. The comparison suggests that each batch of crystallization product was predominantly a single polymorph, not a mixture of multiple polymorphs.

Spectroscopic characteristics. IR spectrum of each form of CPAA is shown in Fig. 7. All three forms show similar IR spectra, but subtle differences are observed for the various forms as indicated in Table 4.

For all three forms of CPAA, the Raman spectrum was measured for comparison (Fig. 8). Differences are subtle yet distinguishable (Table 5).

The vibrational spectra show the effect of the intramolecular hydrogen bond between NH and O=C. The NH stretch is at a lower frequency of around 3326, 3342, 3324 cm^{-1} for forms **I**, **II** and **III**, respectively, the carboxyl C=O stretch is at 1619 cm^{-1} for forms **I** and **II**, and 1604 cm^{-1} for form **III**, and the C–Cl stretch is at 756.0 cm^{-1} for forms **I** and **II**, and 759.2 cm^{-1} for form **III**.

Solvent can dictate polymorphism preference in many polymorphic systems.[45–48] The predominant conformation in the solution may be conserved in the solid state. Since the polymorph formation of CPAA seems to show some solvent selectivity, we measured the UV-vis spectra in several solvents. The data are shown in Fig. 9. All three solutions have similar UV-vis curves. Two peaks are observed in the spectrum for each solution, and the subtle

Table 4 Characteristic IR peaks of the three polymorphs of CPAA

	N–H stretch	Carboxyl O–H stretch and aromatic C–H stretch	Carboxyl C=O stretch	Aromatic C=C stretch	C–Cl stretch
Form **I**	3328.5	3005.2–2560.5	1665.2	1570.8 1510.1 1429.7	756.0
Form **II**	3328.5	3025.7–2553.9	1658.6	1570.8 1513.1 1429.7	756.0
Form **III**	3328.5	3059.4–2553.9	1665.2	1570.8 1503.6 1422.4	759.2

Table 5 Characteristic Raman peaks of the three polymorphs of CPAA

	N–H stretch	Carboxyl O–H stretch and aromatic C–H stretch	Carboxyl C=O stretch	Aromatic C=C stretch	C–Cl stretch
Form I	3325.6	3090.9–3063.9	1600.9	1507.6 1465.8 1406.5	756.9
Form II	3342.1	3084.0–3048.7	1619.6	1508.1 1467.2 1403.8	754.3
Form III	3324.1	3097.4–3053.4	1604.5	1511.6 1471.1 1425.5	765.7

difference lies in the maximum absorption wavelength and extinction coefficient of the peak corresponding to the n → π* excitation of the carboxyl C=O group: λ_{max} = 361.9 nm and ε = 5.30 × 10^3 L mol^{-1} cm^{-1} in $CHCl_3$, λ_{max} = 359.6 nm and ε = 7.20 × 10^3 L mol^{-1} cm^{-1} in CH_2Cl_2 and λ_{max} = 359.6 nm and ε = 4.33 × 10^3 L mol^{-1} cm^{-1} in CH_3COOH, respectively; and that corresponding to π → π* excitation of the substituted benzene ring: λ_{max} = 288.4 nm and ε = 1.23 × 10^4 L mol^{-1} cm^{-1} in $CHCl_3$, λ_{max} = 286.8 nm and ε =1.78 × 10^4 L mol^{-1} cm^{-1} in CH_2Cl_2, λ_{max} = 284.9 nm and ε = 9.90 × 10^3 L mol^{-1} cm^{-1} in CH_3COOH. The UV-vis spectra seem to reflect the small conformational difference among the three polymorphs of CPAA. The UV-vis spectra are a consequence of the equilibrium of a variety of conformations in the solution rather than the locked conformer in the solid state.

3.3. Computational results

For forms **I**, **II**, and **III**, calculated lattice energies based on the empirically augmented DFT method were −106.70, −104.72, and −194.42 kJ mol^{-1}, respectively. The energy difference between form **III** and forms **I** and **II** is much higher than 6 kJ mol^{-1}, which is in agreement with the observation that conformational polymorphs have higher lattice energies difference.[43] The results suggest the stability order to be **III** > **I** > **II** with form **III** being the most stable one, which agrees with the observation that form **II** converts into form **III** when heated. The density values indicate a ranking order of forms **II** > **I** > **III** with form **II** being the densest (Table 2). All three forms have similar calculated densities at 90 K (**I**: 1.432 g cm^{-3}; **II**: 1.451 g cm^{-3}; and **III**: 1.419 g cm^{-3}). While form **II** has a higher density than that of form **I**, its lattice energy is higher than that of form **I** which might be due to the hydrogen bond difference between the two forms, since form **I** has a shorter and more linear hydrogen bond than form **II**. Nonetheless, the small energy difference between forms **I** and **II** should not be regarded as evidence of which is more stable, since there is uncertainty inherent to the computational methods employed (which may range from a few kJ mol^{-1} to a few kCal mol^{-1}, or even higher). Also it should be pointed out that the computation implicitly assumed a temperature of 0 K, whereas the densities are based on the structures measured at 90 K, and the DSC experiments were performed at elevated temperatures, which could cause the discrepancy.

CPAA is a conformationally flexible molecule, for which polymorphism could arise from its intrinsic conformational flexibility. The conformational scan conducted over τ for a single CPAA molecule is illustrated in Fig. 10. The global minima of τ are identified at ±43 and ±143 due to the symmetry of the benzene ring. The conformer of form **III** lies at the exact minimum, the other four conformers from forms **I** and **II** are located near the minima (*i.e.*, well within the energy well), and the conformers reside in two different energy valleys. Thus it appears that the polymorphic system is of conformational polymorphism, not merely due to conformational adjustment.[49] The torsion angle of all five conformations is listed in Table 6.

Hirshfeld surface analysis. The Hirshfeld analysis results are shown in Fig. 11. It is evident that in all fourteen potential molecular contacts, hydrogen–hydrogen contacts predominate, contributing 38.5, 43.2 and 31.0% of

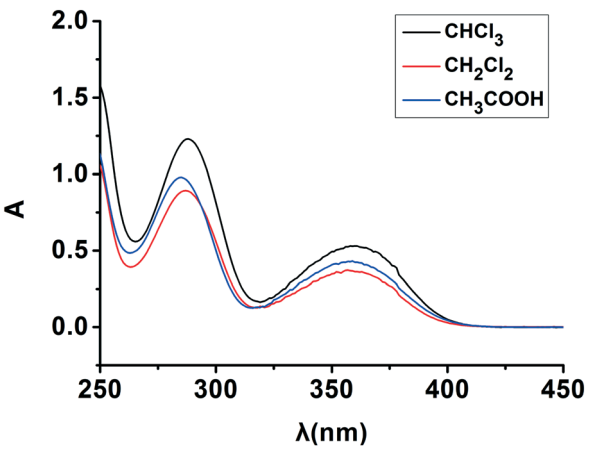

Fig. 9 UV-vis spectra of CPAA in different solvents.

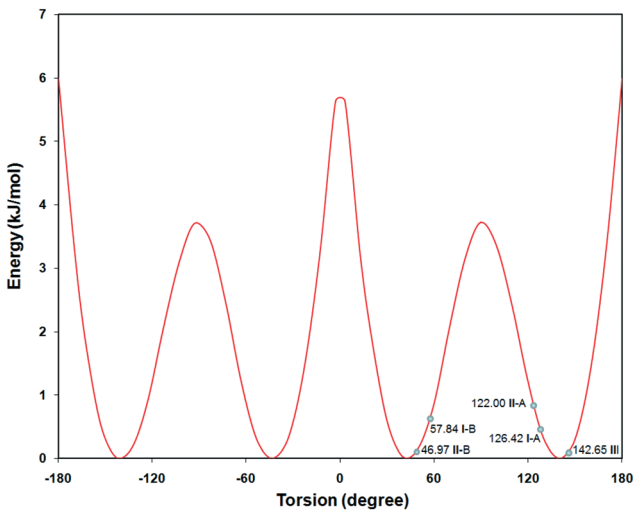

Fig. 10 Conformation scan of single CPAA molecule.

Table 6 Torsion angle of the conformers

Conformer	Torsion angle (C1–N7–C8–C9/C13) (°)
I-A	−55.24/126.42
I-B	57.84/−125.12
II-A	−60.92/122.00
II-B	46.97/−138.13
III	−40.30/142.65

the overall intermolecular interactions in forms **I**, **II** and **III**, respectively. The second most significant intermolecular interaction is C···H, resulting in 20.7, 15.8, and 24.6% of the sum of intermolecular interactions in the individual forms. In addition, H···Cl and H···O interactions also contribute significantly to the total intermolecular interactions. Surprisingly, the Cl···Cl interaction is present only in form **III**, and provides only marginal contribution. Taken together, the crystal structures were stabilized by a variety of interactions.

4. Conclusions

CPAA, a fenamic acid with good AKR inhibition, has been found to exist in three solvent-free crystal forms so far. The polymorphs were characterized by structure determination by single-crystal X-ray diffraction, PXRD and spectroscopic methods such as FT-IR and Raman. The polymorphism appears to result from the conformational flexibility of the molecule, as suggested by the conformers in the three modifications and the conformational scan and the $^{sp^2}$CH···Cl

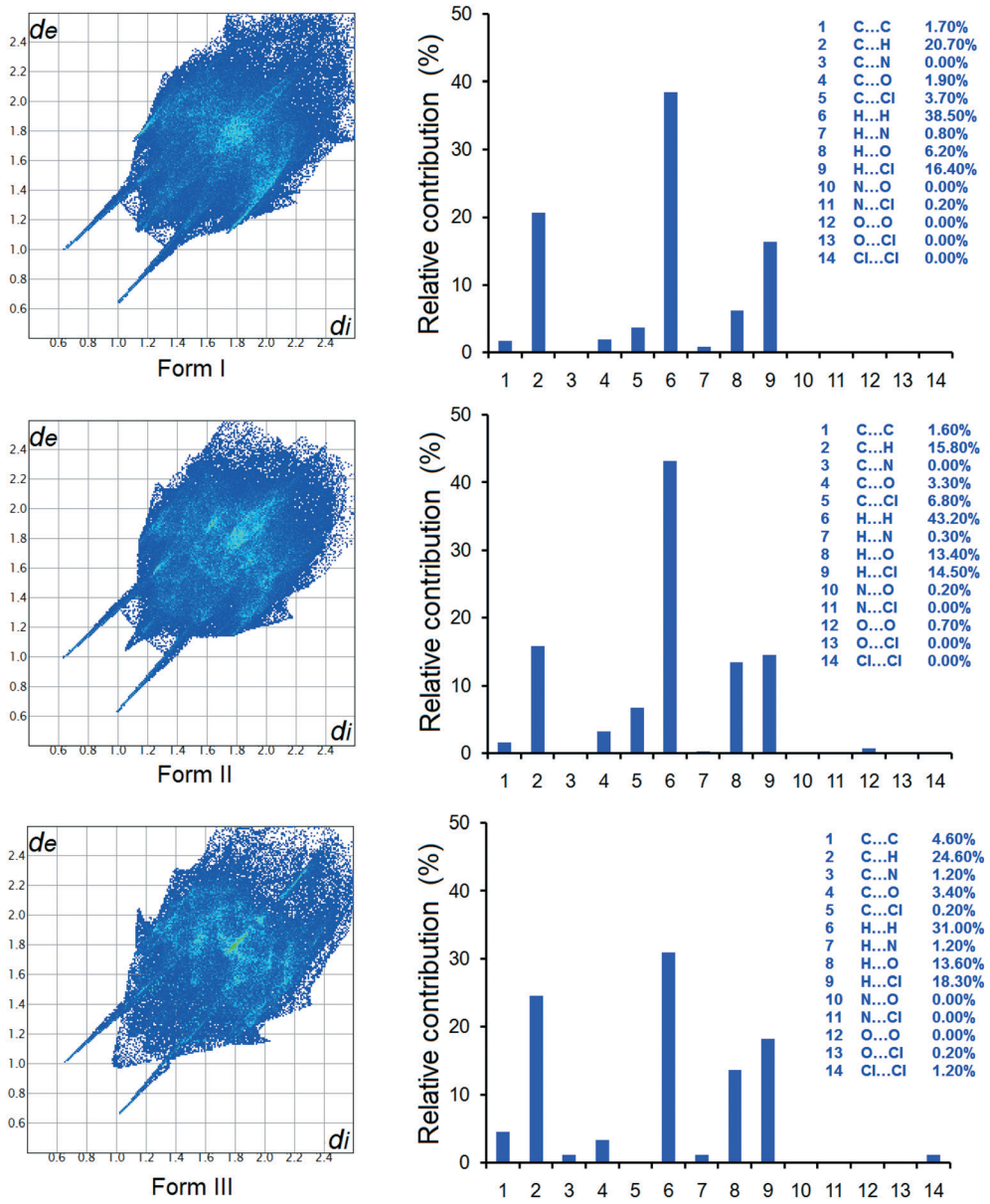

Fig. 11 Hirshfeld surface analysis of the three forms of CPAA.

hydrogen bonds. No halogen bond was observed in any of the three forms. Their phase behaviors were studied by DSC. The metastable form **II** appears to convert into the most stable form **III**. Lattice energies of −106.70, −104.72, and −194.42 kJ mol^{-1} for forms **I** to **III** confirmed the relative stabilities of the polymorphs, and Hirshfeld analysis indicated intermolecular interactions such as H···H, C···H, H···Cl, and H···O contribute significantly to the overall stability of the forms. The knowledge obtained in this study should be valuable to the selection of a suitable form for the formulation of CPAA. We are currently investigating the effects of replacing the chlorine atom by a methyl group.

Acknowledgements

ML and SL thanks Natural Science Foundation of Hubei Province (2014CFB787) and the President's Fund of Wuhan Institute of Technology (CX2016075) for financial support. PPZ acknowledges the financial support by the National Natural Science Foundation of China (Grant No. 21403097) and the Fundamental Research Funds for the Central Universities (lzujbky-2014-182). TL is grateful to NSF for supporting the work (DMR1006364).

References

1 A. Zinellu, C. S. Carru, E. Porqueddu, P. Enrico and L. Deiana, *Eur. J. Pharm. Sci.*, 2005, **24**, 375.
2 L. Fábián, N. Hamill, K. S. Eccles, H. A. Moynihan, A. R. Maguire, L. McCausland and S. E. Lawrence, *Cryst. Growth Des.*, 2011, **11**, 3522.
3 C. M. Ulrich, J. Bigler and J. D. Potter, *Nat. Rev. Cancer*, 2006, **6**, 130.
4 C. Wolf, S. Liu, X. Mei, A. T. August and M. D. Casimir, *J. Org. Chem.*, 2006, **71**, 3270.
5 A. Martín, R. F. Pellón, M. Mesa, M. L. Docampo and V. Gómez, *J. Chem. Res.*, 2006, **9**, 561.
6 M. C. Byrns and T. M. Penning, *Chem.-Biol. Interact.*, 2009, **178**, 221.
7 T. M. Penning, S. Steckelbroeck, D. R. Bauman, M. W. Miller, Y. Jin, D. M. Peehl, K. M. Fung and H. K. Lin, *Mol. Cell. Endocrinol.*, 2006, **248**, 182.
8 D. R. Bauman, S. I. Rudnick, L. M. Szewczuk, Y. Jin, S. Gopishetty and T. M. Penning, *Mol. Pharmacol.*, 2005, **67**, 60.
9 P. Wangemann, M. Wittner, H. C. Englert, H. J. Lang, E. Schlatter and R. Greger, *Pfluegers Arch.*, 1986, **407**, 128.
10 D. Sharples, *J. Pharm. Pharmacol.*, 1982, **34**, 681.
11 W. C. McCrone, in *Physics and Chemistry of the Organic Solid State*, ed. D. Fox, M. M. Labes and A. E. Weissberger, Interscience Publishers, New York, 1965, vol. 2, p. 725.
12 A. Nangia, *Acc. Chem. Res.*, 2008, **41**, 595.
13 F. Kato, M. Otsuka and Y. Matsuda, *Int. J. Pharm.*, 2006, **321**, 18.
14 V. López-Mejías and A. J. Matzger, *Cryst. Growth Des.*, 2015, **15**, 3955.
15 V. Lópezmejías, J. W. Kampf and A. J. Matzger, *J. Am. Chem. Soc.*, 2012, **134**, 9872.
16 P. P. Bag and C. M. Reddy, *Cryst. Growth Des.*, 2012, **12**, 2740.
17 S. S. Kumar and A. Nangia, *Cryst. Growth Des.*, 2014, **14**, 1865.
18 *Polymorphism in Pharmaceutical Solids*, ed. H. G. Brittain, Marcel Dekker, New York, 1999.
19 S. R. Byrn, R. R. Pfeiffer and J. G. Stowell, *Solid State Chemistry of Drugs*, SSCI, Inc., West Lafayette, IN, 2nd edn, 1999.
20 K. Gnanaguru, N. Ramasubbu, K. Venkatesan and V. Ramamurthy, *J. Org. Chem.*, 1985, **50**, 2337.
21 G. R. Desiraju and R. Parthasarathy, *J. Am. Chem. Soc.*, 1989, **111**, 8725.
22 S. L. Price, A. J. Stone, J. Lucas, R. S. Rowland and A. E. Thornley, *J. Am. Chem. Soc.*, 1994, **116**, 4910.
23 O. Navon, J. Bernstein and V. Khodorkovsky, *Angew. Chem., Int. Ed. Engl.*, 1997, **36**, 601.
24 P. Metrangolo, H. Neukirch, T. Pilati and G. Resnati, *Acc. Chem. Res.*, 2005, **36**, 386.
25 D. Das and G. R. Desiraju, *Chem. – Asian J.*, 2006, **1**, 231.
26 Nonius, *Collect*, Nonius BV, Delft, the Netherlands, 2002.
27 Z. Otwinowski and W. Minor, in *Methods in Enzymology: Macromolecular Crystallography, Part A*, ed. C. W. Carter Jr. and R. M. Sweet, Academic Press, New York, 1997, vol. 276, p. 307.
28 G. M. Sheldrick, *Acta Crystallogr., Sect. A: Found. Crystallogr.*, 2008, **64**, 112.
29 G. M. Sheldrick, *Acta Crystallogr., Sect. C: Struct. Chem.*, 2015, **71**, 3.
30 R. Dovesi, R. Orlando, A. Erba, C. M. Zicovich-Wilson, B. Civalleri, S. Casassa, L. Maschio, M. Ferrabone, M. De La Pierre, P. D'Arco, Y. Noel, M. Causa, M. Rerat and B. Kirtman, *Int. J. Quantum Chem.*, 2014, 1287.
31 T. Li and S. Feng, *Pharm. Res.*, 2006, **23**, 2326.
32 S. Feng and T. Li, *J. Chem. Theory Comput.*, 2006, **2**, 149.
33 S. F. Boys and F. Bernardi, *Mol. Phys.*, 1970, **19**, 553.
34 F. L. Hirshfeld, *Theor. Chim. Acta*, 1977, **44**, 129.
35 M. A. Spackman and D. Jayatilaka, *CrystEngComm*, 2009, **11**, 19.
36 S. K. Wolff, D. J. Grimwood, J. J. McKinnon, M. J. Turner, D. Jayatilaka and M. A. Spackman, *CrystalExplorer (Version 3.1)*, University of Western Australia, 2012.
37 M. C. Etter, *Acc. Chem. Res.*, 1990, **23**, 120.
38 M. C. Etter, J. C. Macdonald and J. Bernstein, *Acta Crystallogr., Sect. B: Struct. Sci.*, 1990, **46**, 256.
39 J. Bernstein, R. E. Davis, L. Shimoni and N. L. Chang, *Angew. Chem., Int. Ed. Engl.*, 1995, **34**, 1555.
40 E. Arunan, G. R. Desiraju, R. A. Klein, J. Sadlej, S. Scheiner, I. Alkorta, D. C. Clary, R. H. Crabtree, J. J. Dannenberg, P. Hobza, H. G. Kjaergaard, A. C. Legon, B. Mennucci and D. J. Nesbitt, *Pure Appl. Chem.*, 2011, **83**, 1637.
41 G. R. Desiraju, *CrystEngComm*, 2007, **9**, 91.
42 A. J. Cruz-Cabeza, S. M. Reutzel and J. Bernstein, *Chem. Soc. Rev.*, 2015, **44**, 8619.
43 A. Bauer-Brandl, E. Marti, A. Geoffroy, A. Poso, J. Suurkuusk, E. Wappler and K. H. Bauer, *J. Therm. Anal. Calorim.*, 1999, **57**, 7.

44 E. V. Boldyreva, S. G. Arkhipov, T. N. Drebushchak, V. A. Drebushchak, E. A. Losev, A. A. Matvienko, V. S. Minkov, D. A. Rychkov, Y. V. Seryotkin, J. Stare and B. A. Zakharov, *Chem. – Eur. J.*, 2015, **21**, 15395.
45 M. Kitamura, T. Hara and M. Takimoto-Kamimura, *Cryst. Growth Des.*, 2006, **6**, 1945.
46 R. M. Vrcelj, H. G. Gallagher and J. N. Sherwood, *J. Am. Chem. Soc.*, 2001, **123**, 2291.
47 I. Weissbuch, V. Y. Torbeev, L. Leiserowitz and M. Lahav, *Angew. Chem., Int. Ed.*, 2005, **44**, 3226.
48 A. Blagus and B. Kaitner, *J. Chem. Crystallogr.*, 2007, **37**, 473.
49 A. J. Cruz-Cabeza and J. Bernstein, *Chem. Rev.*, 2014, **114**, 2170.

